

Combustion of Butyl Carbitol using Supported Palladium Catalysts

L. S. Feio¹, J. C. Escritori¹, F. B. Noronha²  and C. E. Hori¹ 

(1) School of Chemical Engineering, Federal University of Uberlandia, Av. João Naves de Ávila, 2160, Bloco 1K, Campus Santa Mônica, Uberlandia, MG, 38400-902, Brazil

(2) National Institute of Technology, INT, Av. Venezuela 82, Rio de Janeiro, RJ, 20081-310, Brazil

 **F. B. Noronha**
Email: fabiobel@int.gov.br

 **C. E. Hori (Corresponding author)**
Email: cehori@ufu.br

Abstract Palladium catalysts supported on CeO₂, Ce_{0.75}Zr_{0.25}O₂, ZrO₂, TiO₂, Nb₂O₅, Al₂O₃ were studied on the total oxidation of butyl carbitol. Several techniques were used to characterize the samples such as diffuse reflectance spectroscopy (DRS), temperature programmed reduction (TPR), cyclohexane dehydrogenation and CO temperature programmed desorption (TPD). DRS and TPR results revealed the presence of bulk PdO and PdO with strong interaction with the support. The catalytic tests showed the following order for decreasing activity:

Pd/Ce_{0.75}Zr_{0.25}O₂ > Pd/CeO₂ > Pd/TiO₂ > Pd/Nb₂O₅ > Pd/Al₂O₃ > Pd/ZrO₂. However, when the *turnover frequency* (TOF) was calculated, all the samples had similar values.

Keywords Butyl carbitol - Volatile organic compounds - Palladium - Combustion

1 Introduction

During the 20th century, the growing human population associated to the correspondent increase in the industrial activities has caused severe pollution problems throughout the world. Even nowadays, large quantities of pollutants are still released to the atmosphere or to water streams untreated. Fortunately, several countries are now regulating the emission of pollutants from both stationary (industries) and mobile (cars, trucks, etc.) sources [1, 2]. Among all kinds of atmospheric pollutants special attention must be given to carbon monoxide, nitrogen oxides, sulfur compounds and the volatile organic compounds (VOCs). These substances are critical not just due to their toxic characteristics but also because of the large quantities that are produced and released to the atmosphere by industrial and agricultural activities [3, 4].

Volatile organic compounds are known as one of the biggest classes of atmospheric pollutants. They are used in a variety of processes and their replacement is very difficult in the majority of these activities [5–8]. One of these applications is the use of a variety of oxygenated compounds as paint solvents in order to achieve the desired viscosity. Among these solvents, one must notice: a compound called butyl carbitol (diethylene glycol mono butyl ether) because it is widely used as solvent for automotive paints [9]. When this solvent evaporates inside the paint booths, it generates a gas stream that has a small concentration of this solvent in air. However, it has been demonstrated that this

solvent can cause severe respiratory problems to humans and animals, even at very low concentrations [10].

In order to comply with the environmental regulations already in place, both in Europe and in North American countries, it is necessary to eliminate this solvent from the air stream. Since the pollutant is present in very low concentrations, one of the best treatment options is the thermal or catalytic incineration [11–15]. The majority of the industrial processes still use thermal incineration, despite its high energy costs due to operation at high temperatures, and the formation of dangerous byproducts such as nitrogen oxides. The use of catalysts to burn VOCs has become increasingly advantageous since it is able to reduce the necessary temperature to transform the pollutants into carbon dioxide and water [2]. On the other hand, in order to use a catalyst efficiently, a previous study about its activity, selectivity and stability is mandatory. Very often, the lack of this kind of information restrains the use of catalysts by industries [11, 16].

Usually the catalysts that are used to eliminate VOCs are noble metal based due to their high activity and stability. Among all the noble metals, palladium has been widely studied for the incineration of pollutants not just because its high activity for oxidation reactions but also due to its lower cost when compared to other noble metals [5, 11, 17–19]. We could not find any studies in the literature about the catalytic elimination of butyl carbitol. Therefore, we decided to investigate the performance of supported palladium catalysts on the total oxidation of butyl carbitol.

2 Experimental

2.1 Catalyst Preparation and Characterization

CeO₂ and ZrO₂ supports were obtained from the calcination of (NH₄)₂Ce(NO₃)₆ (Aldrich) and Zr(OH)₄ (MEL), at 773 K during 1 h with a heating rate of 5 K/min. Ceria–zirconia mixed oxide (Ce/Zr ratio = 3) was prepared by co-precipitation of (NH₄)₂Ce(NO₃)₆ (Aldrich), ZrO(NO₃)₂ (Aldrich), in the presence of excess NH₄OH (Merck). The precipitate was washed with de-ionized water and calcined in air at 773 K, for 1 h. Al₂O₃ (Degussa) and TiO₂ (Degussa) were calcined under air flow at 773 K during 1 h with a heating rate of 5 K/min and Nb₂O₅ was obtained from the calcination of niobic acid (CBMM) in air, at 773 K for 1 h.

All the catalysts were obtained by the incipient wetness impregnation of an aqueous solution of Pd(NO₃)₂ (Merck). After the impregnation, the samples were dried at 373 K during 24 h and calcined under an air flow of 50 mL/min at 773 K during 1 h, with a heating rate of 5 K/min. The palladium content of all samples was 1 wt%. The real palladium content was determined by atomic absorption and it was within 10% of the nominal loadings for all the samples.

BET surface area experiments were conducted using a Quantasorb Jr for all the calcined catalysts. The samples (300 mg) were dried at 393 K overnight and the N₂ adsorption was performed at 77 K with N₂ partial pressures between 0.05 and 0.3 atm. For each measurement, at least 5 points were taken. The catalysts presented the following values of BET surface areas: Pd/CeO₂ = 24 m²/g; Pd/Ce_{0.75}Zr_{0.25}O₂ = 105 m²/g; Pd/ZrO₂ = 70 m²/g; Pd/TiO₂ = 49 m²/g; Pd/Nb₂O₅ = 65 m²/g and Pd/Al₂O₃ = 80 m²/g.

X-ray diffraction analyses were done using a RIGAKU diffractometer with a $\text{CuK}\alpha$ radiation. The XRD data were collected for all supports between $2\theta = 20\text{--}65^\circ$ at 0.04 degrees/step with integration times of 1 s/step.

DRS analyses were carried out between 200 and 900 nm, using a Cary 500 spectrometer equipped with an accessory for DRS (Harrick). The supports were used as references during the analysis of the oxidized form of the catalysts.

Temperature Programmed Reduction (TPR) experiments were performed using a quadrupole mass spectrometer (Balzers, model PRISMA-QMS 200). Prior to reduction, the catalysts (200 mg) were dried under He flow at 50 mL/min at 423 K during 30 min with a heating rate 10 K/min. The samples were reduced under a 2% H_2/Ar mixture with a heating rate of 10 K/min up to 773 K. We monitored the masses correspondent to H_2 , H_2O , CO , CO_2 and NO_x , although the last three were not detected.

The dehydrogenation of cyclohexane, which is a structure insensitive reaction, was used to evaluate the dispersion of Pd samples [20]. The reaction was performed at 10^5 Pa in a flow micro-reactor. The sample (10 mg) was previously dried in situ under N_2 flow (30 mL/min) at 393 K during 30 min. Then, the sample was cooled to room temperature and heated in pure hydrogen flow to 773 K at a heating rate of 10 K/min. This temperature was held for 1 h. The sample was then cooled in hydrogen flow to 543 K. The reaction mixture was obtained by bubbling hydrogen through a saturator containing cyclohexane (99.9%) at 285 K ($\text{H}_2/\text{C}_6\text{H}_{12} = 13.2$). The space velocity was (WHSV) 170 h^{-1} and the reaction temperatures varied from 520 to 570 K. At these conditions, no mass transfer or equilibrium limitations were observed. The conversions were kept below 10% in order to guarantee differential conditions. The composition of effluent gas phase was measured by online gas chromatograph equipped with a thermal conductivity detector and Carbowax 20-M in a Chromosorb W column.

2.2 Catalytic Tests

The catalyst pretreatment consisted on drying the sample (30 mg) for 30 min under He flow of 30 mL/min at 423 K (heating rate of 10 K/min). Then, the sample was reduced for 1 h under pure H_2 flow 30 mL/min at 773 K with the same heating rate. The catalytic test was done using a reaction mixture of 1,000 ppm of butyl carbitol in air. This mixture was obtained by passing air through a saturator containing this solvent kept at 339 K. After the reduction, the temperature was lowered to 573 K in helium flow and then the reaction mixture was fed to the reactor. In order to obtain a light-off curve, the reaction temperature was raised until 100% conversion was obtained. The reactor effluent was analyzed using a GC equipped with a thermal conductivity detector and a 3 m Porapak R column. No partial oxidation products were detected.

3 Results and Discussion

3.1 Characterization

Figure 1 presents the XRD profiles of the supports ZrO_2 , $\text{Ce}_{0.75}\text{Zr}_{0.25}\text{O}_2$ and CeO_2 . Profile A is correspondent to ZrO_2 and shows that there are two zirconia crystalline phases: tetragonal (JCPDS—14-534) e monoclinic (JCPDS—13-307). On the other hand, profile C shows that ceria exhibits the lines characteristics of the cubic phase (JCPDS—4-0593) [21–24]. For ceria-zirconia sample (profile B), it can be observed

that the peaks are similar to the ones obtained for ceria. However, there is a displacement of the peaks to higher 2θ positions. Comparing the higher intensity peaks, for CeO_2 the positions are $2\theta = 28.6^\circ$ and 33.2° and for $\text{Ce}_{0.75}\text{Zr}_{0.25}\text{O}_2$ these peaks appear at $2\theta = 29.0^\circ$ and 33.5° . Accordingly to the literature, this shift in the position of the peaks is probably due to the decrease on the ceria's lattice parameter caused by the addition of zirconium in the lattice [22]. The lack of peaks characteristic of zirconia phases in the $\text{Ce}_{0.75}\text{Zr}_{0.25}\text{O}_2$ profile is an indication that the cubic phase of ceria was maintained after the addition of zirconium and that probably a ceria-zirconia solid solution was obtained. This result is consistent with several studies in the literature [22–24]. For the other supports, the XRD showed the presence of $\gamma\text{-Al}_2\text{O}_3$, a mixture of anatase (80%) and rutile (20%) phases for TiO_2 , and a mixture of T and TT phases for Nb_2O_5 .

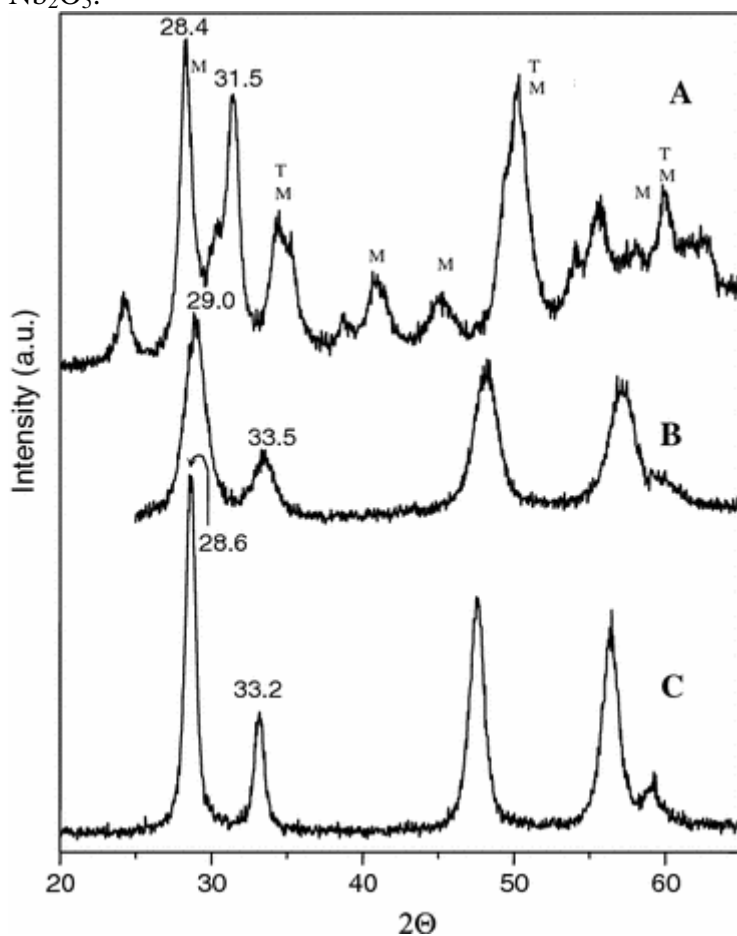


Fig. 1 X-Ray diffraction profiles for A-Pd/ CeO_2 , B-Pd/ $\text{Ce}_{0.75}\text{Zr}_{0.25}\text{O}_2$, C-Pd/ ZrO_2 samples, T – zirconia tetragonal phase, M- zirconia monoclinical phase

The DRS spectra of different Pd samples are shown in Fig. 2. It can be observed that all catalysts presented a band around 470 nm. Pd/ TiO_2 and Pd/ Nb_2O_5 also exhibits a band around 420 nm, while Pd/ ZrO_2 and Pd/ Al_2O_3 showed another one at 380 nm. In addition, Pd/ ZrO_2 had an extra band at 247 nm.

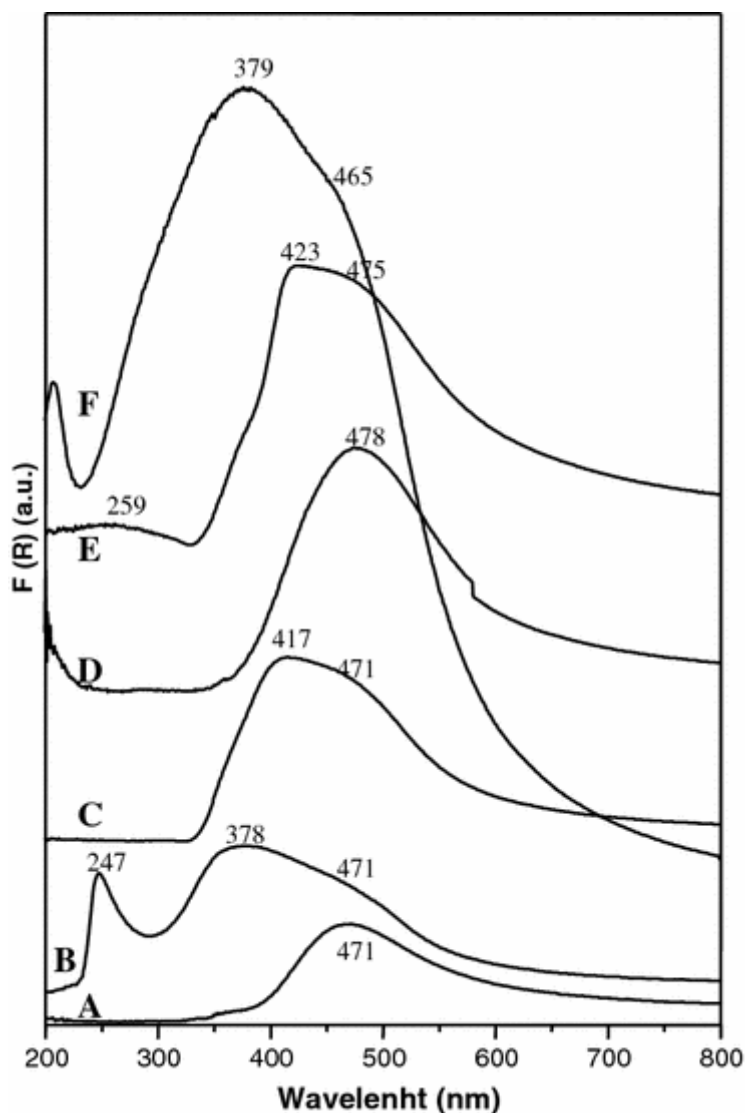


Fig. 2 DRS spectra for Pd supported catalysts. A-Pd/CeO₂, B-Pd/ZrO₂, C-Pd/Nb₂O₅, D-Pd/Ce_{0.75}Zr_{0.25}O₂, E-Pd/TiO₂, F-Pd/Al₂O₃

According to the literature, the bands around 400 and 470 nm can be attributed to the palladium oxide d–d transition. Rakai et al. [25] studied unsupported and alumina supported palladium catalysts using DRS. For the unsupported samples, they verified the presence of a large band between 380 and 500 nm. For Pd/Al₂O₃, the authors observed a band around 450 nm, when they used palladium chloride as a precursor, and another band at 460 nm when the precursor was palladium acetyl acetonate. These bands were attributed to the d–d transition of Pd⁺². Lomot et al. [26] also verified the presence of these d–d transition bands in Pd/SiO₂ calcined at different temperatures. Noronha et al. [27] used UV–visible diffuse reflectance spectroscopy to study Pd/Al₂O₃ and Pd/Nb₂O₅ catalysts. The DRS spectrum of the Pd/Al₂O₃ sample exhibited 3 bands at 287, 325, and 458 nm, which were attributed to metal-ligand charge transfer, Pd(H₂O)₄²⁺ complex and d–d transition, respectively. The Pd/Nb₂O₅ sample spectrum showed only one band around 407 nm. According to the authors, the band at 287 nm was due to the presence of PdO_xCl_y species on the Pd/Al₂O₃ sample whereas the Pd/Nb₂O₅ sample showed only PdO particles corresponding to the band at 407 nm. The bands around 380 nm that were present in the spectra obtained for Pd/Al₂O₃ and Pd/ZrO₂ samples can be attributed to the presence of water in the coordination sphere of

palladium $[Pd(H_2O)_4]^{2+}$ [25]. The appearance of isolated bands around 247 nm as the ones verified for Pd/ZrO₂ may be due to the charge transfer from the oxygen of the support to the d orbitals of palladium [28].

Figures 3 and 4 present the reduction profiles of all the catalysts. It can be noticed that all samples had H₂ consumption at room temperature. Several studies in the literature attributed this peak to the reduction of palladium oxide (PdO) and to the adsorption and absorption of hydrogen on the metallic palladium [29–32]. These results are consistent with the DRS data of these catalysts which presented bands around 400 and 470 nm attributed to d–d transitions, revealing the presence of large particles of PdO.

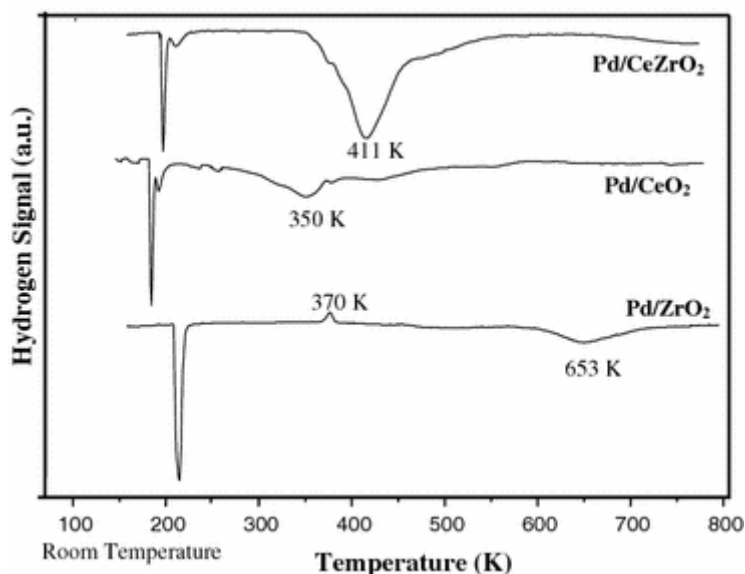


Fig. 3 Temperature programmed reduction profiles for Pd/CeO₂, Pd/ZrO₂, and Pd/Ce_{0.75}Zr_{0.25}O₂ catalysts

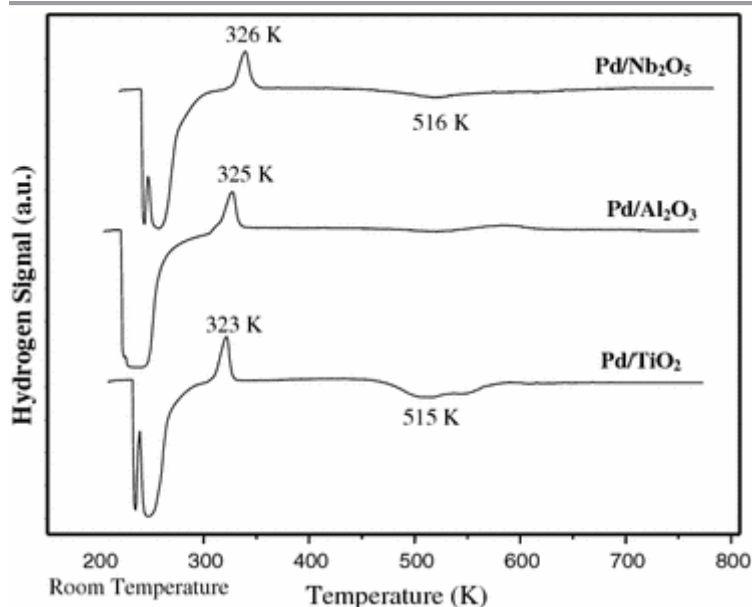


Fig. 4 Temperature programmed reduction profiles for Pd/TiO₂, Pd/Al₂O₃ and Pd/Nb₂O₅ catalysts

As the temperature is increased, new peaks of hydrogen consumption can be observed. For Pd/ZrO₂ (Fig. 3), there is a negative peak around 350 K. This same peak is observed for Pd/Nb₂O₅, Pd/Al₂O₃ and Pd/TiO₂ samples (Fig. 4). Usually this feature is attributed

to the desorption of the weakly adsorbed hydrogen on the metal surface and to the decomposition of the palladium hydride formed at room temperature [30, 33]. The hydrogen consumption at higher temperatures can be attributed to the reduction of small particles of PdO and to the reduction of the support [34]. For instance, it can be seen in Fig. 4, there was a small consumption of hydrogen for Pd/Nb₂O₅, around 516 K and for Pd/TiO₂, around 515 K. These consumptions at higher temperatures have been usually attributed to the partial reduction of Nb₂O₅ and TiO₂ [27, 30]. On the other hand, for Pd/Ce_{0.75}Zr_{0.25}O₂ and Pd/CeO₂ these peaks were observed in Figure 3 at 411 and 350 K, respectively. As the total hydrogen consumption (Table 1) for these samples is above the theoretical value necessary to reduce all the palladium oxide (94 μmol of H₂/g_{cat}), it is correct to affirm that there is a partial reduction of the support (Ce⁺⁴ to Ce⁺³) for these catalysts. Although zirconia is difficult to reduce, the presence of zirconium in the ceria lattice favors the reduction of Ce⁺⁴ to Ce⁺³. According to the literature, the presence of this atom generates defects, increasing the oxygen mobility in the ceria lattice [20, 21]. This can explain the high hydrogen consumption observed for Pd/Ce_{0.75}Zr_{0.25}O₂. This result agrees with the ones observed by Luo and Zheng [34] for Pd/Ce_{0.50}Zr_{0.50}O₂ and by Hori et al. [24] for platinum supported on CeO₂, ZrO₂ and Ce_{0.75}Zr_{0.25}O₂. For Pd/ZrO₂ sample, the hydrogen consumption was lower than the theoretical value for the reduction of palladium. Since zirconia is very difficult to reduce, the small peak observed at 640 K may be attributed to the reduction of small particles of PdO that had higher interaction with the support.

Table 1 H₂ consumption during temperature programmed reduction experiments

Catalyst	μ moles of H ₂ g catalyst	
	Room temperature	Total
Pd/CeO ₂	10	126
Pd/Ce _{0.75} Zr _{0.25} O ₂	18	383
Pd/ZrO ₂	11	65
Pd/Al ₂ O ₃	110	110
Pd/Nb ₂ O ₅	80	110
Pd/TiO ₂	71	108

The values of reaction rate and metal dispersion are presented in Table 2. The results show that all the catalysts have low dispersions, between 9 and 14%. These metal dispersion values are in agreement with TPR and DRS experiments, which revealed the presence of large PdO particles [32, 35].

Table 2 Cyclohexane reaction rates and Pd dispersions

Sample	Reaction rate (mol/g.*h)	Dispersion(%)
Pd/CeO ₂	0.0113	9
Pd/Ce _{0.75} Zr _{0.25} O ₂	0.0199	11
Pd/ZrO ₂	0.0309	14
Pd/Al ₂ O ₃	0.0190	11
Pd/Nb ₂ O ₅	0.0198	11
Pd/TiO ₂	0.0317	14

3.2 Catalytic Tests

The light off curves for the reaction of total oxidation of butyl carbitol are shown in Fig. 5. Pd/Ce_{0.75}Zr_{0.25}O₂ catalyst reached a conversion of butyl carbitol of 95% at 488 K.

This is more than 80 K of temperature reduction when comparing with the less active catalyst, Pd/ZrO₂, which had a conversion of 95% only at 574 K. The temperatures necessary to reach 50% of conversion (light-off temperatures) are shown in Table 3 and the order of increasing light-off temperatures is:

Pd/Ce_{0.75}Zr_{0.25}O₂ > Pd/CeO₂ ≈ Pd/TiO₂ > Pd/Nb₂O₅ ≈ Pd/Al₂O₃ ≈ Pd/ZrO₂. The stability of all the samples was tested by repeating a high temperature point and a low temperature point after the light off experiment. All the samples were approximately stable. Table 3 also presents the results of turnover frequencies (TOF) calculated at 448 K, using conversions between 12 and 15%. All the samples had very similar TOF values, around $4.5 \times 10^{-3} \text{ s}^{-1}$.

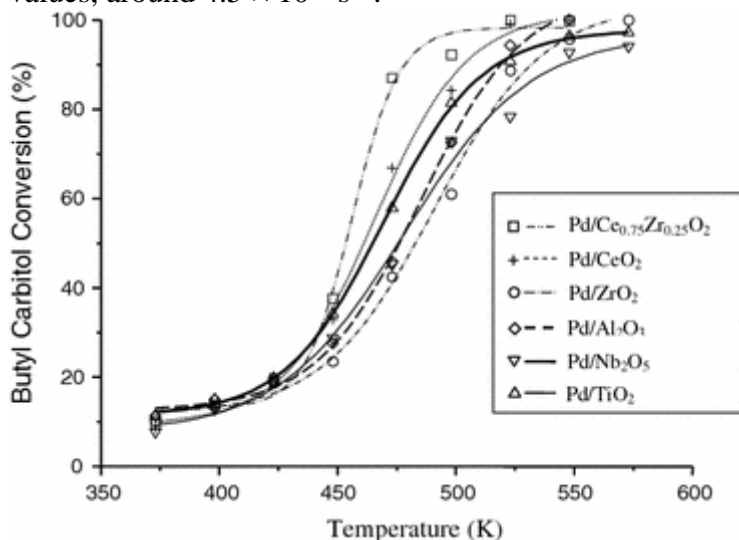


Fig. 5 Butyl carbitol conversion as a function of temperature for Pd supported catalysts after reduction at 573 K for 1 hour

Table 3 Light-off temperatures and turnover frequencies (TOF) obtained during the total oxidation of butyl carbitol using supported palladium catalysts

Catalyst	Light-off Temperature (K)	TOF (s ⁻¹)
Pd/Ce _{0.75} Zr _{0.25} O ₂	453	$4.6 \cdot 10^{-3}$
Pd/CeO ₂	462	$5.7 \cdot 10^{-3}$
Pd/TiO ₂	466	$3.9 \cdot 10^{-3}$
Pd/Al ₂ O ₃	478	$4.9 \cdot 10^{-3}$
Pd/Nb ₂ O ₅	476	$4.2 \cdot 10^{-3}$
Pd/ZrO ₂	483	$3.5 \cdot 10^{-3}$

In the literature, the effect of the particle size on the catalytic hydrocarbon oxidation is controversial. A strong dependence between the activity and the particle size has been reported [36]. This effect has been extensively discussed on the total oxidation of methane. These studies are scarcer for other hydrocarbons such as benzene and for oxygenated compounds like butanol, ethyl acetate [3]. However we were unable to find a study about particle size dependence on butyl carbitol oxidation.

Chin and Resasco [22] reported a strong dependence of the TOF for methane oxidation with Pd particle size, taking into account literature data. They observed that the activity increased as dispersion decreased. Also Papefthimiou et al. [36] studied the effect of

metal dispersion on the intrinsic activity of the oxidation of different volatile organic compounds (benzene, butanol, ethyl acetate) on Pt/Al₂O₃ and Pd/Al₂O₃ catalysts. Benzene and ethyl acetate oxidation over Pt/Al₂O₃ catalyst revealed to be structure sensitive reactions. The TOF of ethyl acetate oxidation enhanced 25 times as Pt particle increased from 1 to 30 nm. On the other hand, the TOF of butanol oxidation was independent of Pt particle size. In the case of Pd catalyst, the TOF of all three compounds was practically independent of dispersion.

Accordingly to the literature [36], the particle size effect on the total oxidation of hydrocarbons is directly correlated to the PdO species that are present on the catalyst surface and with the strength of the Pd–O bond. In general, there are two types of palladium oxide: bulk PdO and PdO with a strong interaction with the support. The first kind is present in samples with low metal dispersions, while the second one is characteristic of catalysts with higher dispersions, which would provide a stronger interaction with the support. These two different PdO species present distinct oxygen adsorption and desorption properties [37]. Accordingly to Fugimoto et al. [33], small PdO_x particles have higher interaction with the support and would have a stronger Pd–O bond than larger particles. This Pd–O bond would cause a decrease in the stability and density of oxygen vacancies that are necessary during the oxidation reaction. Therefore, the catalysts with lower dispersion would present a higher turnover frequency.

Besides the particle size effect, the catalytic activity of hydrocarbon oxidation can also be influenced by the nature of the support [22]. Yazawa et al. [38] studied the effect of the nature of support on the propane combustion over Pd supported on Al₂O₃, SiO₂, ZrO₂, SiO₂–Al₂O₃, MgO and SO₄²⁻–ZrO₂. After reaction at 773 K, XRD and XPS analyses revealed that the presence of metallic palladium and palladium oxide was a function of the oxygen/propane ratio. XPS spectra of Pd/ZrO₂, Pd/Al₂O₃, Pd/SiO₂–Al₂O₃ exhibited the peak of Pd3d_{5/2} at 335.0–335.1 eV, which is assigned to metallic palladium and at 336.5–336.6 eV corresponding to PdO. Furthermore, the catalytic activity was significantly affected by the oxidation state of palladium. The highest activity was observed on the catalysts containing partially oxidized palladium. According to the authors, the nature of the support affects the resistance of palladium oxidation and consequently the catalytic activity. Acidic supports prevent the palladium oxidation.

Noronha et al. [27] also observed a support effect on the propane oxidation over Pd/Al₂O₃, Pd/Nb₂O₅ and Pd/Nb₂O₅/Al₂O₃ catalysts. The niobia addition promoted the propane oxidation at lower temperatures than Pd/Al₂O₃ catalyst. In fact, infrared spectroscopy of adsorbed CO on Pd/Al₂O₃ and Pd/Nb₂O₅/Al₂O₃ catalysts after propane oxidation showed that the amount of Pd⁰ and Pd²⁺ species was function of Nb₂O₅ loading. These results suggested that the partially reduced niobia species prevented the palladium oxidation.

The support may also take part in the mechanism of oxidation reactions [22]. In this study, de Leitenburg et al. investigated the oxidation of isobutane using ceria and ceria-zirconia oxides. Although the presence of zirconia did not affect the conversion, the selectivity to isobutene was significantly higher for ceria-zirconia sample. This effect was attributed to higher oxygen mobility in the ceria-zirconia lattice caused by the presence of zirconia.

In our work, all catalysts exhibited the same Pd dispersion. Therefore, the particle size effect could be ruled out and the results could be evaluated as a function of the nature of support. However, the TOF were the same, regardless the support. A difference was observed on the light off temperatures of the catalysts, which was around 30 K between the most (Pd/Ce_{0.75}Zr_{0.25}O₂) and less (Pd/ZrO₂) active catalysts. It is worth noting that the activity order was the same of the hydrogen consumption on the TPR experiment. This correlation between activity and support reduction degree suggests that the support may play a role on the reaction mechanism. In fact, it is well established that Ce_{0.75}Zr_{0.25}O₂ and CeO₂ have a high oxygen exchange capacity, which is associated to the ability of cerium to act as an oxygen buffer by storing/releasing O₂ due to the Ce⁴⁺/Ce³⁺ redox couple [21]. The incorporation of ZrO₂ into CeO₂ lattice promotes the CeO₂ redox properties. The presence of ZrO₂ strongly increases the oxygen vacancies of the support, increasing its reducibility. This result is in agreement with our TPR measurements. One possible explanation is that these oxides could be participating in the reaction as oxygen donors and promoting the oxidation through the Max-van-Krevelen mechanism.

In order to try to identify changes in the palladium phases present during the total oxidation of butyl carbitol, the following experiment was carried out: we decided to measure the palladium dispersion of a catalyst before and after the reaction. To simplify the experimental work, the dispersion was estimated using CO chemisorption and the sample selected was Pd/ZrO₂, since it presented higher metal dispersion than the others and it does not have the problem of adsorption of CO on the support. The sample was reduced in pure H₂ with the same procedure used during catalytic tests and submitted to the reaction mixture with reaction temperatures varying from 373 and 573 K. After the reaction, the sample was cooled to room temperature in air flow and then purged with He. Only then, the second CO adsorption was performed. Considering a stoichiometry of CO/Pd = 1, the results show an initial dispersion value of 20% and after the reaction it dropped to 3%. This result is a good indication that although metallic palladium is present, the predominant palladium phase during the reaction is PdO. Probably, the interchangeability between Pd⁰/PdO is crucial for the catalytic activity during the total oxidation of butyl carbitol.

4 Conclusions

This study showed that supported palladium catalysts are active for the total oxidation of butyl carbitol and the active phase is probably Pd⁰/PdO. All the samples presented similar and very low palladium dispersions, so we could not verify particle size effects on the catalytic activity. DRS and TPR experiments confirmed the presence of large PdO particles on the catalysts surface. Pd/Ce_{0.75}Zr_{0.25}O₂ and Pd/CeO₂ were the most active samples probably due to the participation of ceria in the reaction through a Max-van-Krevelen type of mechanism.

References

1. Dobson ID (1994) Prog Org Coat 24:55

2. Dégé P, Pinard L, Magnoux P, Guisnet M (2001) *Comptes Rendus de l'Académie des Sciences - Series IIC - Chemistry* 4(1):41
3. Papaefthimiou P, Ioannides T, Verykios XE (1997) *Appl Catal B* 13:175
4. Tidahy, Siffert S, Lamonier J-F, Zhilinskaya EA, Aboukaïs A, Yuan Z-Y, Vantomme A, Su B-L, Canet X, De Weireld G, Frere M, N'Guyen TB, Giraudon J-M, Leclercq G (2006) *Appl Catal A: Gen* 310:69
5. Centi G (2001) *J Mol Catal A: Chem* 173(1–2):287
6. Ferreira RSG, de Oliveira PGP, Noronha FB (2004) *Appl Catal B: Environ* 50(4):243
7. Aranzabal A, González-Marcos JA, Ayastuy JL, González-Velasco JR (2006) *Chem Eng Sci* 61(11):3564
8. Brayner R, Cunha DS, Bozon-Verduraz F (2003) *Catal Tod* 78(1–4):419
9. Armor JN (1992) *Appl Catal B* 1:221
10. Beach JR, Raven J, Ingram C, Bailey M, Johns D, Walters EH, Abraham M (1997) *Eur Resp J* 10:563
11. Noordally E, Richmond JR, Tahir SF (1993) *Catal Tod* 17:359
12. Engleman VS (2000) Engleman Associates, Inc. San Diego, California, p 433
13. Khan FI, Ghoshal AKr, Loss J (2000) *Prev Proc Ind* 13:527
14. Heck RM, Farauto RJ (1995) *Catalytic air pollution control: commercial technology*. Van Nostrand Reinhold, New York, p 147

15. Spivey JJ (1987) *Ind Eng Chem Res* 26:2165
16. Dégé Ph, Pinard L, Magnoux P, Guisnet M (2000) *Appl Catal B: Environ* 27(1):17
17. Ferrandon M, Björnbohm E (2001) *J Catal* 200(1):148
18. Garcia T, Solsona B, Cazorla-Amorós D, Linares-Solano A, Taylor SH (2006) *Appl Catal B: Environ* 62(1–2):66
19. Giraudon JM, Elhachimi A, Wyrwalski F, Siffert S, Aboukaïs A, Lamonier J-F, Leclercq G (In Press) *Appl Catal B: Environ* (Corrected Proof, Available online 16 April 2007)
20. Feio LSF, Hori CE, Damyanova S, Noronha FB, Cassinelli WH, Marques CMP, Bueno JMC (2007) *Appl Catal A: Gen* 316(1):107
21. Trovarelli A (1996) *Catal Rev-Sci Eng* 38:439
22. Leitenburg C, Trovarelli A, Llorca J, Cavani F, Bini G (1996) *Appl Catal A* 139:161
23. Terribile D, Trovarelli A, Leitenburg C, Primavera A, Dolcetti G (1999) *Catal Today* 47(1–4): 133
24. Hori CE, Permana H, Simon NGKY, Brenner A, More K, Rahmoeller KM, Belton DN (1998) *Appl Catal B* 16:105
25. Rakai A, Tessier D, Bonzon-Verduraz F (1992) *New J Chem* 16:869
26. Lomot D, Juszczak W, Pielaszek J, Kaskur Z, Bakuleva NT, Karpinski Z (1995) *New J Chem* 19:263
27. Noronha FB, Aranda DAG, Ordine AP, Schmal M *Catal Today* 57:275

28. Zou W, Gonzáles RD (1992) Catal Today 12:73
29. Noronha FB, Schmal M (1991) Appl Catal 78:125
30. Okzan US, Kumthekar MW, Karakas G (1998) Catal Today 40:3
31. Pereira MM, Noronha FB, Schmal M (1993) Catal Today 16:407
32. Gaspar AB, Dieguez LC (2000) Appl Catal A 201:241
33. Fugimoto IK, Ribeiro FH, Avalos-Borja M, Iglesia E (1998) J Catal 179:431
34. Luo MF, Zheng XM (1999) Appl Catal A 189:15
35. Panpranot J, Tangjitwattakorn O, Praserttham P, Goodwin JG Jr (2005) Appl Catal A:Gen 292:322
36. Chin HY, Resasco ED (1999) Roy Soc Chem 14
37. Chou P, Vannice MA (1987) J Catal 105:342
38. Yazawa Y, Takagi N, Yoshida H, Komai S, Satsuma A, Tanaka T, Yoshida S, Hattori T (2002) Appl Catal A 233:113